Check for updates

Targeted and efficient activation of channelrhodopsins expressed in living cells *via* specifically-bound upconversion nanoparticles†

Kanchan Yadav,‡[a,b,c] Ai-Chuan Chou,‡[d] Rajesh Kumar Ulaganathan,[a,b,c] Hua-De Gao,[a,e] Hsien-Ming Lee,*[e] Chien-Yuan Pan [ID] *[d,f] and Yit-Tsong Chen [ID] *[a,c]

Optogenetics is an innovative technology now widely adopted by researchers in different fields of biological sciences. However, most light-sensitive proteins adopted in optogenetics are excited by ultraviolet or visible light which has a weak tissue penetration capability. Upconversion nanoparticles (UCNPs), which absorb near-infrared (NIR) light to emit shorter wavelength light, can help address this issue. In this report, we demonstrated the target selectivity by specifically conjugating the UCNPs with channelrhodopsin-2 (ChR2). We tagged the V5 epitope to the extracellular N-terminal of ChR2 (V5-ChR2m) and functionalized the surface of UCNPs with NeutrAvidin (NAv-UCNPs). After the binding of the biotinylated antibody against V5 onto the V5-ChR2m expressed in the plasma membrane of live HEK293T cells, our results showed that the NAv-UCNPs were specifically bound to the membrane of cells expressing V5-ChR2m. Without the V5 epitope or NAv modification, no binding of UCNPs onto the cell membrane was observed. For the cells expressing V5-ChR2m and bound with NAv-UCNPs, both 488 nm illumination and the upconverted blue emission from UCNPs by 980 nm excitation induced an inward current and elevated the intracellular Ca^{2+} concentration. Our design reduces the distance between UCNPs and light-sensitive proteins to the molecular level, which not only minimizes the NIR energy required but also provides a way to guide the specific binding for optogenetics applications.

[a]*Department of Chemistry, National Taiwan University, No. 1, Sec. 4, Roosevelt Road, Taipei 106, Taiwan. E-mail: ytcchem@ntu.edu.tw*
[b]*Nano Science and Technology Program, Taiwan International Graduate Program, Academia Sinica and National Taiwan University, Taipei, Taiwan*
[c]*Institute of Atomic and Molecular Sciences, Academia Sinica, P.O. Box 23-166, Taipei 106, Taiwan*
[d]*Department of Life Science, National Taiwan University, No. 1, Sec. 4, Roosevelt Road, Taipei 106, Taiwan. E-mail: cypan@ntu.edu.tw*
[e]*Institute of Chemistry, Academia Sinica, Nankang, Taipei, 11529, Taiwan. E-mail: leehm1@gate.sinica.edu.tw*
[f]*Graduate Institute of Brain and Mind Sciences, National Taiwan University, No. 1, Sec. 4, Roosevelt Road, Taipei 106, Taiwan*

†Electronic supplementary information (ESI) available: Electron microscopy and X-ray diffraction characterization of UCNPs, a ninhydrin assay for the presence of amine groups on UCNPs, a Bradford assay for NAv-UCNPs, the zeta potentials on different surfaces of UCNPs, hydrodynamic sizes of UCNPs with different surface modifications, localization of V5-ChR2m on the cell membrane, specific binding of NAv-UCNP to V5-ChR2m in the cell lysate, specific binding of NAv-UCNPs to the V5-ChR2m on the cell membrane, and the Experimental section. See DOI: 10.1039/c7nr03246c

‡These authors equally contributed to this work.

Introduction

Optogenetics, the integration of the two important techniques of optics and genetics, opens a new avenue for accentuating or attenuating the well-defined functions in the designated cells of live animals.[1] Optogenetics involves two steps, first, the expression of a light-sensitive protein in the specific cells, and second, the illumination of those cells at appropriate wavelengths to activate light-sensitive protein-conjugated ion channels or enzymes.[2] Channelrhodopsin-2 (ChR2) is a transmembrane protein found in green algae (*Chlamydomonas reinhardtii*).[3] Upon excitation with blue light, ChR2 (maximum response peaked at ~460 nm) undergoes a conformational change of the incorporated retinal from all-*trans* to 13-*cis*-retinal and opens the channel pore for cation passage.[4] After light-excitation, retinal relaxes to its all-*trans* form within milliseconds, closing the pores and stopping the ion flow.[5]

ChR2 and other similar proteins with different ion selectivities have been widely adopted by neuroscientists to characterize circuit connections in the nervous system and to verify the effectiveness of therapies for neurological disorders.[6] By acti-

vating or inhibiting neurons expressing light-sensitive channels in the central nucleus of the amygdala, one can regulate anxiety levels in murine models.[7] With optogenetic control of neuronal activity in the basal ganglia, researchers could alleviate or exacerbate Parkinson's disease symptoms in rodents.[8,9] By expressing ChR2 in the dopaminergic neurons of Rhesus monkey, researchers can control the reward-learning behavior.[10] Additionally, the expression of targeted genes could be controlled by conjugating a DNA-binding protein with a light-sensitive transcription factor-binding protein.[11] Henceforth, upon illumination, optogenetics could provide precise temporal and spatial manipulation of activities in cells expressing light-sensitive proteins.

Despite the advantages of optogenetics, one major limitation of this technique is that visible and ultraviolet (UV) light cannot penetrate deeply into biological soft tissues unless an invasive guide is used to introduce light to the target tissues expressing light-sensitive proteins. Lanthanide-doped up-conversion nanoparticles (UCNPs), which absorb NIR radiation and emit visible light, may serve as a non-invasive light source for deep-tissue optogenetic purposes. UCNPs have excellent biocompatibility, chemical and photostability, minimal auto-fluorescence, and low toxicity.[12–14] The physical (*e.g.*, size, emission wavelength, *etc.*) and chemical properties (*e.g.*, solubility, surface charge, *etc.*) of UCNPs are easily tailored by controlling reaction conditions and surface modifications, respectively.[12–17] Recently, UCNPs have been employed in various biological applications, such as imaging,[18–22] photodynamic therapy,[22–25] biomolecule delivery and detection,[26–28] fluorescence resonance energy transfer (FRET),[29–32] photoactivation of various biomolecules,[33,34] and control of the cellular signal transduction pathways[35] and cell adhesion.[36]

Recently, UCNPs with different modifications, such as poly-lactic-*co*-glycolic acid-UCNPs,[37] collagen/poly-L-lysine-UCNPs,[38] UCNP-embedded poly(methyl-methacrylate),[39] and silica-UCNPs,[40] have been applied to activate various types of ChR2s. However, these modified UCNPs have no specific targeting and are not in close proximity at the molecular level to the light-sensitive ChR2s. Instead, UCNPs are randomly biodistributed[40] or coated on a substrate that is distant away from the ChR2s, hence requiring a higher UCNP/ChR2 stoichiometric ratio to provide sufficient energy for the ChR2 activation.[37–39] To minimize or prevent the collateral damage on healthy tissues, nanoparticle-based therapeutics should have specific targeting to pathologic tissues.[41–48] and also necessitate low NIR power, thus avoiding thermal damage.[49,50] Therefore, to improve UCNP-based photoactivation of ChR2, a design involving the uniform distribution of UCNPs within tissues and specific molecular recognition of UCNPs to the ChR2 should be a preferred approach that can create an effective and less invasive nanotransducer system.

Taking the target specificity and low NIR power into account, our present study is about constructing an NIR-activating UCNP-conjugated ChR2 system on the cell surface to bring a UCNP in close proximity to the ChR2. We first functionalized the UCNPs with NeutrAvidin (referred to as NAv-UCNPs) (Scheme 1) and employed a molecular biology technique to tag a V5 epitope at the extracellular N-terminal of a ChR/H134R (ChR2), which had also been fused with mCherry at the intracellular C-terminal (ChR2m). The whole construct was referred to as V5-ChR2m (Scheme 2). Subsequently, the V5-ChR2m was expressed in the cell membrane and was tagged with a biotinylated antibody against the V5 epitope (referred to as bV5-Ab). Consequently, the NAv-UCNPs could recognize and link efficiently with the bV5-Ab through the biotin–avidin interaction. With this design, low NIR power was enough to activate the NAv-UCNP-bound V5-ChR2m as evidenced by the ionic current through the conjugated channel and the elevation of the intracellular Ca^{2+} concentration ($[Ca^{2+}]_i$). These results demonstrate the feasibility of this experimental design for the target-specific binding of UCNPs to ChR2 and efficient activation of the conjugated channel by low NIR illumination power in live cells.

Results and discussion

Experimental design and UCNP characterization

To functionalize the UCNPs for the NIR-optogenetics approach, we first tuned the dopant concentration in UCNPs
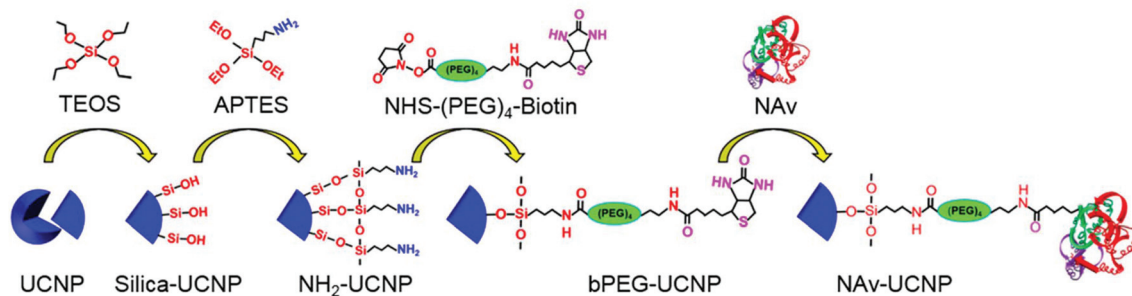
Scheme 1 Surface modifications of UCNPs. UCNPs were modified sequentially with tetraethyl orthosilicate (TEOS) and aminopropyltriethoxysilane (APTES) to generate the amine-functionalized silica surface. An *N*-hydroxysuccinimide-(polyethylene-glycol)$_4$-biotin (NHS-(PEG)$_4$-biotin) conjugates with the exposed −NH$_2$ group on the silica-UCNP surface (to form bPEG-UCNPs) for the subsequent binding of NeutrAvidin (NAv) *via* the strong biotin−avidin interaction.
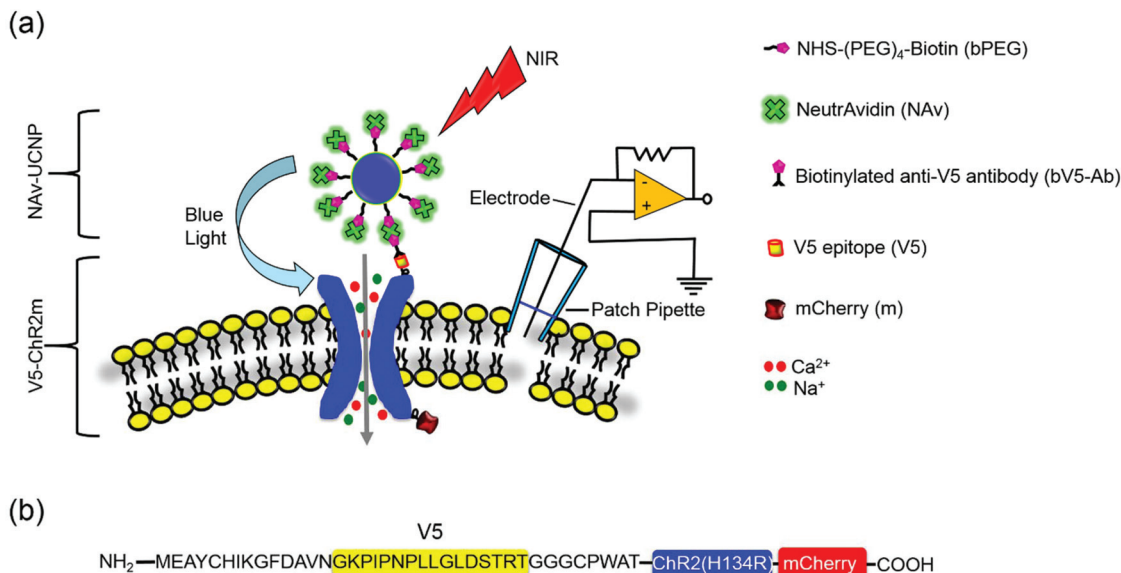
Scheme 2 Schematic illustrations of the experimental design. (a) Binding of NAv-UCNPs to ChR2 on a cell membrane. ChR2 is fused with the fluorescent protein of mCherry at the intracellular C-terminal and is tagged with a V5 epitope at the extracellular N-terminal (referred to as V5-ChR2m). After the binding of bV5-Ab to the V5-ChR2m, the NAv-UCNPs then anchor to bV5-Ab and transfer the upconverted blue light upon 980 illumination to activate the conjugated ion channels of ChR2. (b) The protein sequence at the N-terminal of the V5-ChR2m system.
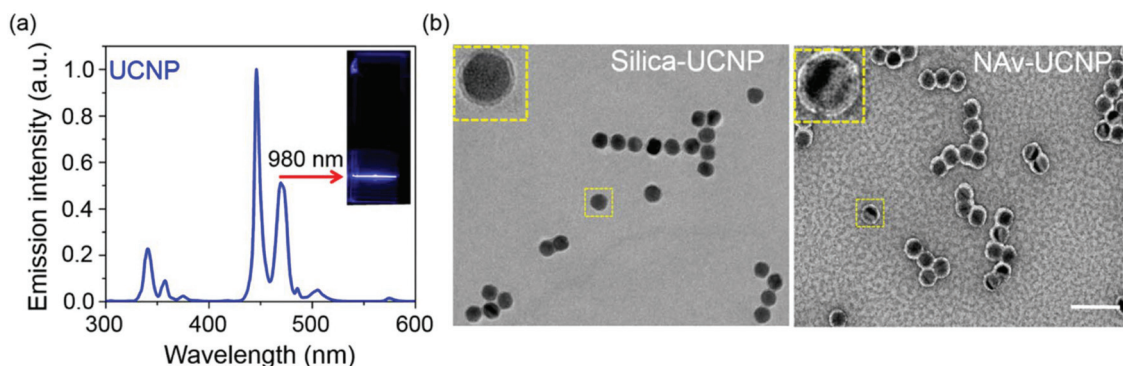

Fig. 1 Characterization of UCNPs. (a) The emission spectrum of UCNPs (NaYF$_4$:30% Yb^{3+}, 1% Tm^{3+}) was scanned in cyclohexane solution (1 mg mL^{-1}) under 980 nm excitation at 1 W. The inset shows a luminescence image of the UCNPs in a cuvette upon 980 nm illumination, where the arrow indicates the direction of an incident laser beam. (b) TEM images of the UCNPs were taken after silica coating (silica-UCNPs) and NeutrAvidin modification (NAv-UCNPs), in which the samples were negatively stained with 2% uranyl acetate. The insets show enlarged images of the corresponding UCNPs. Scale bar: 100 nm (applicable to both panels).

to 30% Yb^{3+} and 1% Tm^{3+} to achieve luminescence at 453 and 474 nm, respectively (Fig. 1a), which overlap with the spectral absorption of ChR2 (~460 nm).[4,51] Second, the UCNPs were coated with polyethylene glycol (PEG) to enhance the colloidal stability, prevent particulate aggregation in a biological buffer solution, and reduce non-specific binding for subsequent cellular experiments.[47,52,53] Third, the conjugation between NAv-UCNPs and V5-ChR2m shortened the distance from UCNPs to ChR2 (Schemes 1 and 2), compared to previous reports.[37–39] Therefore, integrating the UCNPs with ChR2 not only compensates the disadvantage of traditional short-wavelength acti-

vation of ChR2 but also provides an effective approach in manipulating optogenetic experiments.

The detailed procedures to generate NAv-UCNPs along with their respective characterization are described in the Experimental section and ESI (sections S1–S5 and S9 in the ESI†). A ninhydrin assay was used to determine the concentration of amine groups on the UCNP surface to be 84 nmol mg^{-1}. The transmission electron microscopy (TEM) images of NAv-UCNPs revealed a bright layer surrounding the UCNPs in contrast to the bare silica-coated UCNPs (referred to as silica-UCNPs) (Fig. 1b), indicating successful conjugation of the

NAv-protein on the UCNP surface. In addition, the zeta potential varied after each surface modification (Fig. S4 in the ESI†), demonstrating the distinctive surface charges on the different functionalized molecules.

V5-ChR2m localizes in the cell membrane

To verify the localization and the orientation of V5-ChR2m in HEK293T cells, we used a primary antibody against the V5 epitope (V5-Ab) followed by a secondary antibody conjugated with fluorescent Alexa Fluor-488 (Fig. S6 in the ESI†). The fluorescence was observed only at the cell boundary of the live cells expressing V5-ChR2m, but not ChR2m, indicating that the V5 epitope was in the extracellular region (Fig. S6a in the ESI†). After cell fixation and membrane permeabilization, the antibody can reach the V5 epitope at the lumen of the endoplasmic reticulum (ER) and Golgi body;[54] therefore, the fluorescence signals were present in both plasma membranes and intracellular organelles in the cells expressing V5-ChR2m (Fig. S6b in the ESI†). For the cells expressing ChR2m which has no V5 epitope, there was no fluorescence signal observed, indicating the specific binding of the antibody to the V5 epitope. Therefore, attaching the V5 epitope to the extracellular N-terminal of ChR2m neither distorts the structural orientation, nor interferes with the membrane targeting capability of ChR2.

Specific binding of NAv-UCNPs to V5-ChR2m

On confirming the specific binding of NAv-UCNPs to the V5-ChR2m in cell lysates using both immuno-dot and pull down assays (section S7 and Fig. S7 in the ESI†), we further investigated this binding of NAv-UCNPs to the V5-ChR2m expressed in live cells. We first incubated live HEK293T cells expressing either V5-ChR2m or ChR2m with bV5-Ab and then the NAv-UCNPs (Fig. 2a, b and Fig. S8 in the ESI†). The successful cellular expressions of V5-ChR2m and ChR2m could be determined by the presence of mCherry fluorescence. As expected, NAv-UCNPs only bound the membrane of the cells expressing V5-ChR2m (in the presence of bV5-Ab), but not in those expressing ChR2m. To further confirm the specificity, several controls were also conducted, in which we either eliminated bV5-Ab (Fig. 2c and d) or used the biotinylated PEG-coated UCNPs (referred to as bPEG-UCNPs) without NAv-modification (Fig. 2e and f) in the binding assay. The UCNP luminescence was not detected in these control groups (Fig. 2c–f), thereby signifying the specific binding of NAv-UCNPs to the cells expressing the bV5-Ab-labeled V5-ChR2m. Recently, Ai *et al.* introduced a copper-free click chemistry approach to conjugate the dibenzyl cyclooctyne-modified UCNPs with membrane glycoproteins tagged with an azido functional group.[55] Their approach, like ours, could anchor the UCNPs to the plasma membrane in close proximity to ChR2. Despite convenience, the method by Ai *et al.* modifies every live cell. In contrast, our design, though required molecular biology to add an epitope at the ChR2, ensures the direct and specific binding of UCNPs to the V5-ChR2m in the cell membrane of transfected cells.

Optogenetic activation of ChR2

(a) Optogenetic activation of ChR2 validated by electrophysiological measurements. To verify that the upconverted blue light from UCNPs could activate V5-ChR2m, we used an electrophysiology technique to measure the inward current *via* the ChR2-conjugated ion channel under NIR illumination (Fig. 3). After the binding of NAv-UCNPs (*via* bV5-Ab) to the live cells expressing V5-ChR2m and forming the NAv-UCNP/V5-ChR2m complex, we patched the cell in whole-cell mode under a voltage clamp with a holding potential of −70 mV (Fig. 3a). By exciting the same patched cells with 488 nm (603 μW mm^{-2}, the direct activation of ChR2) and 980 nm (22.6 mW mm^{-2}, the upconverting activation of ChR2) illumination *via* the optical path of the microscope, we could detect an inward current from the cells expressing V5-ChR2m at both wavelengths (Fig. 3b). To ensure that the observed results were due to the UCNP-assisted ChR2 activation, two different controls were performed. As expected, NAv-UCNPs did not bind the cells expressing either V5-ChR2m without bV5-Ab pretreatment (Fig. 3c and d) or ChR2m (without the V5-modification) with bV5-Ab pretreatment (Fig. 3e and f). The control tests showed that an inward current was induced under the 488 nm illumination, but not under the 980 nm illumination. On average, the 488 nm illumination induced a larger inward current (51 ± 5 pA) than the 980 nm illumination (35 ± 3 pA, $n = 7$, $p < 0.05$) for the cells expressing V5-ChR2m bound with NAv-UCNPs (Fig. 3g). For the cells expressing V5-ChR2m but without NAv-UCNPs binding, the 488 nm, but not 980 nm, excitation induced an inward current of 40 ± 8 pA ($n = 7$, $p < 0.001$). For the cells expressing ChR2m and treated with NAv-UCNPs, an excitation at 488 nm induced an apparent inward current of 61 ± 8 pA ($n = 7$, $p < 0.001$), in contrast to no current observation with 980 nm illumination. These results evidence that the NAv-UCNP conjugation with V5-ChR2m in the cell membrane brings the components in close proximity, where the NIR power at 22.6 mW mm^{-2} is sufficient to activate the ChR2-conjugated ion channels. The results support the fact that our system provides an efficient upconversion of the NAv-UCNPs upon NIR illumination in activating light-sensitive proteins.

(b) Optogenetic activation of ChR2 confirmed by monitoring [Ca^{2+}]$_i$. Because the ChR2-conjugated ion channels are permeable to Ca^{2+} ions,[5] the intracellular Ca^{2+} concentration ([Ca^{2+}]$_i$) in HEK293T cells was monitored with a Ca^{2+}-sensitive dye (Fura-2) to characterize the activation of ChR2 under optogenetic excitation. In this experiment, the expression of HEK293T cells included a voltage-gated Na$^+$ channel (Na$_V$1.4) together with either V5-ChR2m (referred to as V5-ChR2m + Na$_V$1.4), or ChR2m (ChR2m + Na$_V$1.4). As shown in Fig. 4a, after the binding of NAv-UCNPs (*via* bV5-Ab) to the cells expressing V5-ChR2m + Na$_V$1.4, the [Ca^{2+}]$_i$ increased upon 980 nm illumination (at 6.5 mW mm^{-2}). In contrast, because NAv-UCNPs could not bind in both control tests of the ChR2m + Na$_V$1.4 cells pretreated with bV5-Ab (Fig. 4b) and the Na$_V$1.4 cells without V5-ChR2m expression (Fig. 4c), NIR illumination
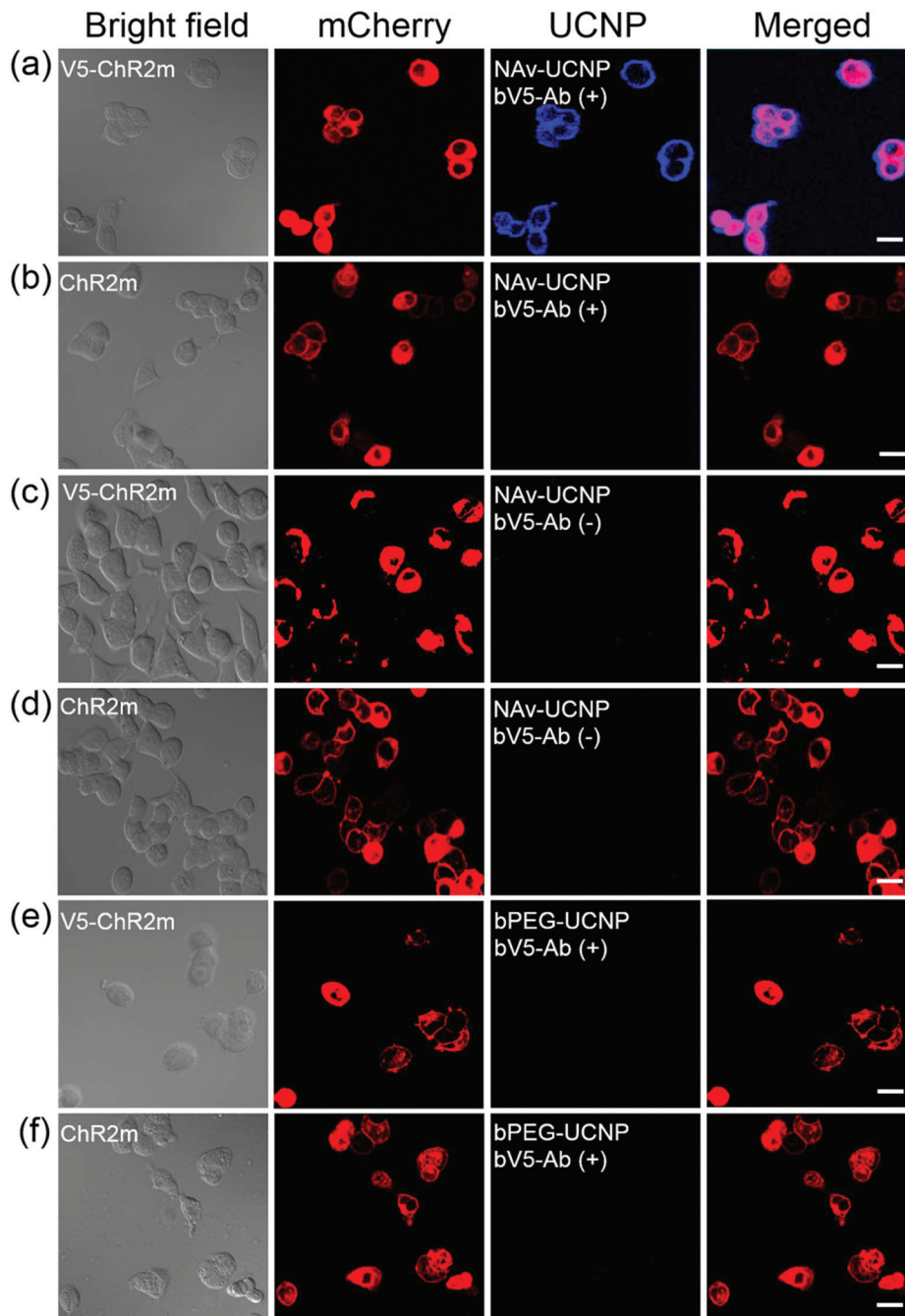
Fig. 2 Specific binding of NAv-UCNPs to V5-ChR2m on a cell membrane. The HEK293T cells expressing V5-ChR2m (a, c, e) or ChR2m (b, d, f) were first stained with bV5-Ab (bV5-Ab (+); a, b, e, f) or without bV5-Ab (bV5-Ab (−); c, d) and then were incubated with (a–d) NAv-UCNPs or (e–f) bPEG-UCNPs. The images shown in each panel from left to right are bright field, mChery fluorescence, blue emission from UCNPs, and the merged fluorescence image from a confocal microscope. Scale bar: 20 μm.

could not elicit any $[Ca^{2+}]_i$ response. As demonstrated in Fig. 4d, the average change of the normalized fluorescence intensity ($\Delta F/F_0$, excited at 340 nm) in the cells expressing V5-ChR2m + $Na_V1.4$ is 0.32 ± 0.02 ($n = 15$), which is significantly higher ($p < 0.001$) than that of the above-mentioned control groups, 0.0024 ± 0.0003 ($n = 15$) for ChR2m + $Na_V1.4$ and 0.0024 ± 0.0005 ($n = 15$) for $Na_V1.4$ (without V5-ChR2m). The co-expression of $Na_V1.4$ was necessary to have an apparent

elevation of $[Ca^{2+}]_i$ in this series of experiments but the exact reason is not clear.

It is important to mention that we applied NIR illumination at 45° from the top of the recording chamber rather than through the optical path of the microscope in activating the UCNPs. Therefore, the NIR had to penetrate the solution (~1 mm) above the cells before reaching the cell surface to excite the UCNPs for ChR2 activation. This experimental
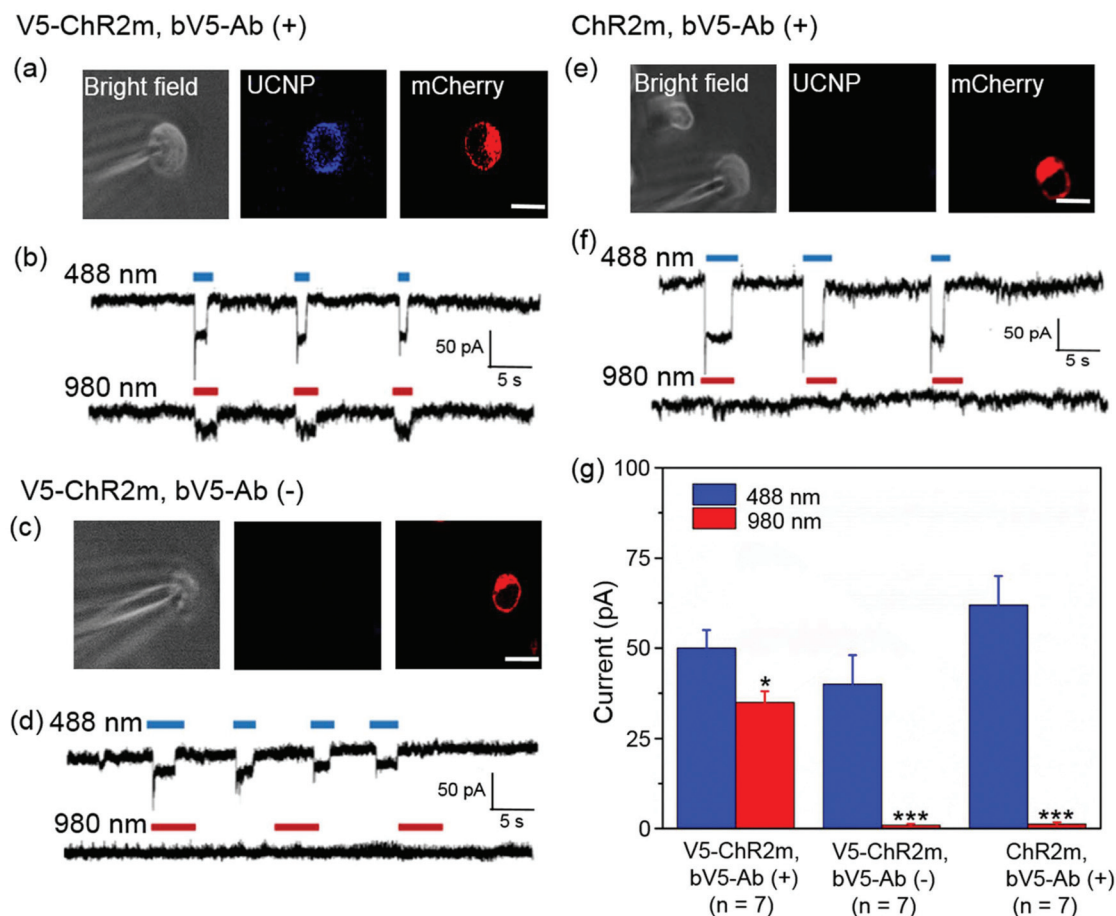
Fig. 3 NIR-upconverted blue light activates the V5-ChR2m. Cells expressing V5-ChR2m (a–d) or ChR2m (e–f) were first stained with (bV5-Ab (+), a–b, e–f) or without (bV5-Ab (−), c–d) bV5-Ab and then incubated with NAv-UCNPs. Subsequently, the cells were whole-cell patched in voltage-clamp mode with a holding potential of −70 mV and the current traces were recorded. (a, c, and e) In the patched cells, the bright field images (left) showed the glass pipette and the patched cells. The middle and right images indicated the UCNP and mCherry fluorescence emissions, respectively. Scale bar: 20 μm. (b, d, and f) The recorded current traces from a patched cell excited by 488 nm (upper panels, blue bars, 603 μW mm^{-2}) or 980 nm (lower panels, red bars, 22.6 mW mm^{-2}) illumination as indicated. (g) The average inward currents induced by 488 or 980 nm illumination. The data presented are the mean ± standard deviation and their statistical significance was determined by using the paired t-test; *: $p < 0.05$ and ***: $p < 0.001$.

design could represent a practical approach for activating UCNPs under tissues for optogenetic applications. Additionally, the low NIR power intensity (6.5 mW mm^{-2}) required in this study for ChR2 activation further demonstrates the importance of the proximity of UCNP–ChR2 at the molecular level. Our system using surface modified UCNPs conferred with target specificity will not only shorten the distance between UCNPs and ChR2 but also reduce the NIR power needed for the ChR2 activation. Thus, a lower UCNP concentration (50 μg ml^{-1}) is enough for the photoactivation of the ChR2 performed in this report than others published elsewhere.[37–40]

Conclusions

In this proof-of-concept report, we first demonstrated the specific binding of the NAv-UCNPs to the V5-ChR2m expressed

on live cells and also in the cell lysates through both immuno-dot and pull-down assays; subsequently, we showed the successful activation of ChR2 by the NIR-upconverted blue light from UCNPs. With distinctive dopants (e.g., Tm^{3+}, Er^{3+}, Ho^{3+}, and Ce^{3+}) within UCNPs, this NIR-activation platform could provide different emissions to activate light-responsive membrane proteins/ion channels with various excitation wavelengths. The direct and specific conjugation of UCNPs with ChR2 brings them in close proximity and facilitates the channel opening under a low NIR power, which in return could minimize the thermal damage and lower the amount of UCNPs employed. Consequently, the demonstrated strategy provides a generic approach that can be duplicated for various light-sensitive proteins and optogenetic experiments with high target specificity and low required illumination power to achieve satisfactory efficacy in activating light-sensitive proteins with NIR illumination.
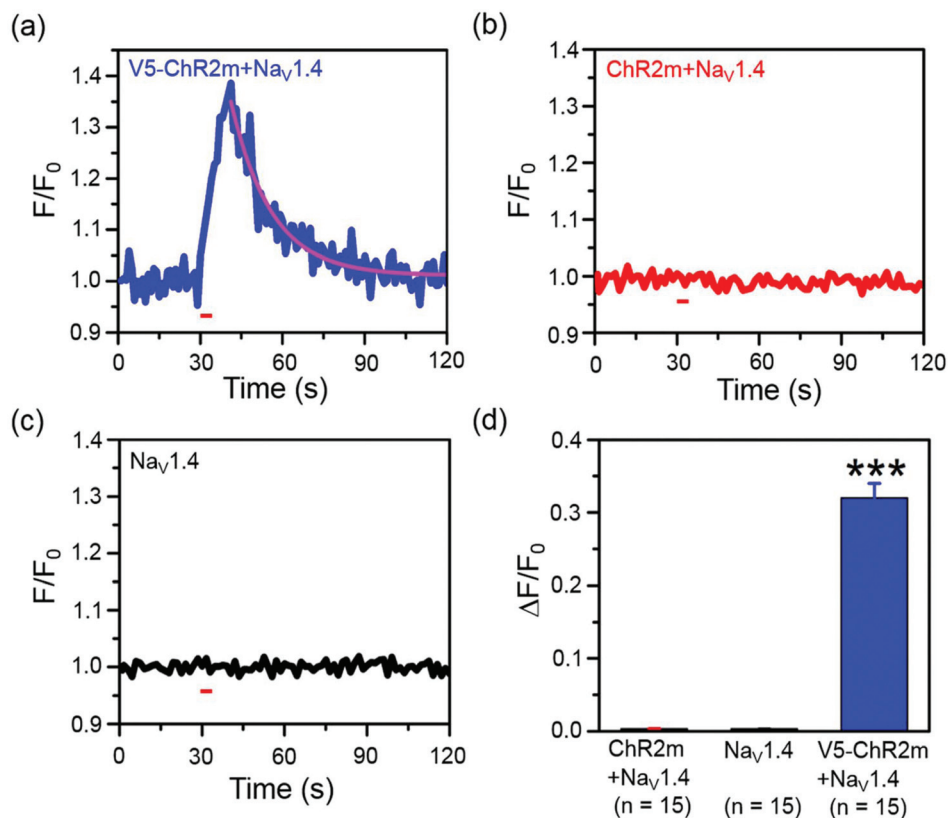
Fig. 4 NIR-upconverted blue light elevates the $[Ca^{2+}]_i$ in the cells conjugated with UCNPs. The HEK293T cells expressing V5-ChR2m + $Na_V1.4$ (a), ChR2m + $Na_V1.4$ (b), and $Na_V1.4$ only (without V5-ChR2m, c) were pretreated with bV5-Ab followed by incubation with NAv-UCNPs. The cells were then loaded with Fura-2 and placed at the stage of an inverted microscope. The changes in $[Ca^{2+}]_i$ were represented by the fluorescence emission excited at 340 nm and the intensity was normalized to the average value before NIR illumination (F/F_0). The decaying phase between 42th and 120th s was fit with a single exponential function and the fit values at the 42th s were adopted as the maximum response. (a–c) The representative F/F_0 traces from the cells transfected with different plasmids. The red bars indicate the period (5 s) of the 980 nm laser excitation (6.5 mW mm^{-2}) with an incident angle of 45-degree from above and directly onto the recording chamber. The pink line in (a) was the fit curve. (d) NIR-induced maximum changes of the fit F/F_0 traces ($\Delta F/F_0$). The data presented are the mean $\pm$ standard deviation and their statistical significance was determined by using one-way ANOVA with a Fisher's *post hoc* test; ***: $p < 0.001$.

Experimental section

Materials

All solvents and reagents used for particle synthesis, spectroscopic characterization, protein modification, and biochemical assays were purchased from Sigma-Aldrich Inc. (St Louis, MO, USA) and were used as received, unless otherwise indicated. The Lipofectamine™ 3000, mouse monoclonal antibodies against the V5 epitope, Dulbecco's modified Eagle's medium, and other chemicals for cell culture were obtained from Invitrogen Inc. (Carlsbad, CA, USA). The Fura-2 acetomethoxylmethyl ester (Fura-2 AM) was purchased from TefLabs (Austin, TX, USA).

Instrumentation

Electron microphotographs were recorded on a JEOL JEM-1400 (120 kV) TEM. X-ray diffraction (XRD) measurements were performed with a Rigaku XRD DMAX-2200VK diffractometer. The zeta potentials of the UCNPs were measured by using a Zetasizer Nano-ZS (Malvern Instrument Inc., UK). Confocal images were obtained by using an LSM 510 Duoscan system (Zeiss Inc., Germany). The upconversion luminescence was measured using a Cary Eclipse fluorescence spectrometer (Varian Inc., CA, USA) coupled with a continuous wave (CW) diode laser at 980 nm with a tunable power range of 0.5–8 W (ChangChun New Industry, China). For the electrophysiology study, patch-clamp studies were performed using an EPC10 amplifier (HEKA Inc. Germany) controlled by using Pulse software while cells were placed on an Olympus IX-71 fluorescence microscope. For $[Ca^{2+}]_i$ measurements, a Ti microscope (Nikon Inc. Japan) equipped with DG4 (Sutter Instrument Inc., CA, USA) was used to provide the excitation wavelength and a charge-coupled device (CCD) camera (Photometrics Inc., AZ, USA) was employed for imaging; the system was controlled by using NIS Element software.

Hydrodynamic size and zeta potential measurement

Displayed in Fig. S4 in the ESI† are the zeta potentials of UCNPs with different surface modifications, including: –silica (−30.5 mV), –NH$_2$ (+31.7 mV), –bPEG (−0.278 mV), and –NAv

(−20.4 mV). The high negative charge on the NAv-UCNPs can be accounted for by the low isoelectric point of NAv (pI = 6.4) in an HBSS buffer (pH = 7.4), which also agrees with the high NAv substitution from the Bradford assay (Fig. S3 in the ESI†). Additionally, as shown in Fig. S5 in the ESI,† the hydrodynamic sizes of different surface-modified UCNPs in buffer are –silica (83.4 nm), –NH$_2$ (85.6 nm), –bPEG (92.5 nm), and –NAv (99.5 nm). The increase in size and the variation of zeta potential indicate the successful modification in each step of functionalization.

Molecular biology

We modified the pcDNA3.1/hChR2(H134R)-mCherry (referred to as ChR2m, a gift from Dr Karl Deisseroth, Addgene Plasmid #20938)[56] construct with a V5 epitope at the N-terminal (referred to as V5-ChR2m) using Phusion DNA polymerase. The primers used for the cloning were 1. 5′-tgcccttgggccaccatggactatggcggc, 2. 5′-ttcattttggggcccgaaggtttt, 3. 5′-ggtaccatggaggcctactgccac, and 4. 5′-tgttgcggtggcggctgcccttgggccacc. We first used primers 1 and 2 to amplify the V5 segment from the pLenti6.2/V5-DEST plasmid and primers 3 and 4 to amplify the ChR2m by polymerase chain reaction (PCR), then mixed the products as the template for another round of PCR using primes 1 and 4 to obtain the V5-ChR2m. The amplified products were then subcloned in the pcDNA3.1 plasmid and sequenced.

Cell culture and transfection

HEK293T cells were maintained in Dulbecco's modified Eagle's medium and were supplemented with 10% of fetal bovine serum. We used the Lipofectamine™ 3000 reagent to introduce plasmids into the cells in accordance with manufacturer's instructions. In brief, we used a total of 2 µg of each plasmid for HEK293T cells grown in a 35 mm dish. Experiments were performed for 24–36 h after transfection.

Protein extraction

To isolate the membrane fraction, we resuspended cells (~10^7) in Hank's balanced salt solution (HBSS, 1.26 mM CaCl$_2$, 5.33 mM KCl, 0.44 mM KH$_2$PO$_4$, 0.50 mM MgCl$_2$, 0.41 mM MgSO$_4$, 138 mM NaCl, 4 mM NaHCO$_3$, 0.3 mM Na$_2$HPO$_4$, and 5.60 mM glucose, pH 7.4) and then centrifuged at 600g for 10 min. Cells were then lysed with RIPA buffer (Bioman, Taiwan). The lysates were then centrifuged at 1000g for 20 min and the supernatant was collected for the immuno-dot and pull-down assays. Finally, the protein concentration was determined with a Bradford kit (Bio-Rad Inc., Hercules, CA, USA).

Binding of NAv-UCNPs to live cells

Live cells were washed with HBSS and incubated in HBSS containing 1% BSA for 5 min. We then washed the cells with HBSS and incubated them in HBSS containing bV5-Ab (1 : 500 dilution) for 30 min. After washing the unbound antibody away with HBSS containing 1% BSA for three cycles, the cells were incubated with NAv-UCNPs (50 µg ml^{-1}) for 30 min followed by washing three times. The cells were then used either for whole-cell electrophysiological experiments and [Ca^{2+}]$_i$ measurement or for confocal imaging analysis.

Immunostaining

For antibody staining on cells, we fixed cells in PBS containing 4% paraformaldehyde for 20 min at room temperature. After a PBS wash, we placed the cells in PBS containing 1% BSA for 1 h; to permeabilize the cell membranes, 0.5% Triton X-100 was added. Triton X-100 can completely permeabilize the cell membranes including the ER and Golgi body; therefore, antibody can access and bind to the antigen inside the lumens of these organelles.[54] We then washed the cells with PBS and incubated them in PBS containing a V5-Ab (1 : 500 dilution, InVitrogen Inc.) at 4 °C overnight. After another PBS wash, we incubated the cells in PBS containing the secondary antibody (goat anti-mouse immunoglobulin) conjugated with Alexa Fluor-488 at a 1 : 2000 dilution for 1 h at room temperature. After washing the unbound antibodies away, we visualized the subcellular fluorescence distribution with a Leica SP5 confocal microscope. For live cell immunostaining, the same protocol was followed as above, except the fixation and Triton X-100 treatments.

Electrophysiological measurement

Cells bound with NAv-UCNPs bathed in HBSS solution were transferred to a recording chamber mounted on the stage of an inverted fluorescence microscope. Electrophysiological recording was performed as reported previously.[57] To activate ChR2, we illuminated the recording chamber with a 488 nm/ 980 nm laser, which was guided through the optical path of the microscope. We measured the applied 980 nm laser intensity by using a thermopile power meter at the stage of an Olympus IX-71 microscope equipped with a 980 nm laser diode at the right-side port of the second tier light path with customized upconversion filter/mirror settings. The output of the NIR laser intensity along the optical path through the microscope objective lens (20×) was measured to be 22.6 mW mm^{-2}. Similarly, the resulting power intensity of the focused blue light through an objective lens (20×) is estimated to be about 603 µW mm^{-2}.

[Ca^{2+}]$_i$ response

Cells transfected with V5-ChR2m together with Na$_V$1.4 were bound with NAv-UCNPs (*via* bV5-Ab) and were loaded with Fura-2 AM (5 µM) for 15 min at 37 °C in HBSS. We then mounted the cells on the stage of a Nikon Ti inverted microscope. The excitation energy (340 nm) for Fura-2 was provided by using a DG4 and the emission was collected with an EM-CCD camera.[58] The system was controlled by the Nikon NIS Elements software. To activate ChR2 activity, we shone the NIR laser for 5 s with an incident angle of 45° from above and directly onto the Nikon Ti inverted microscope stage, but not along the optical path inside the microscope. The fluorescence intensity was normalized to the average value before NIR illumination (F/F_0); to obtain the maximum changes, the decay phase of the F/F_0 trace was fit with a single exponential func-

tion and the maximum fit value was taken as the maximum response.

The laser intensity of 6.5 mW mm^{-2} was obtained using a thermopile power meter at the microscope stage without a recording chamber. During the experiment, cells were placed in a recording chamber containing a buffer of about 1 mm in depth. Therefore, the NIR intensity illuminated on the cell surface should be attenuated by the buffer solution.

Data analysis

Data are presented as the mean ± standard deviation from at least three different experimental batches and were analyzed by one-way ANOVA with a Fisher's *post hoc* test and paired *t*-test. Differences were considered to be significant when the *p*-value was under 0.05.

Acknowledgements

References

1 K. Deisseroth, *Sci. Am.*, 2010, **303**, 48.

2 R. Berry, M. Getzin, L. Gjesteby and G. Wang, *Photonics*, 2015, **2**, 23.

3 O. A. Sineshchekov, K. H. Jung and J. L. Spudich, *Proc. Natl. Acad. Sci. U. S. A.*, 2002, **99**, 8689.

4 J. Y. Lin, M. Z. Lin, P. Steinbach and R. Y. Tsien, *Biophys. J.*, 2009, **96**, 1803.

5 G. Nagel, T. Szellas, W. Huhn, S. Kateriya, N. Adeishvili, P. Berthold, D. Ollig, P. Hegemann and E. Bamberg, *Proc. Natl. Acad. Sci. U. S. A.*, 2003, **100**, 13940.

6 L. Fenno, O. Yizhar and K. Deisseroth, *Annu. Rev. Neurosci.*, 2011, **34**, 389.

7 K. M. Tye, R. Prakash, S. Y. Kim, L. E. Fenno, L. Grosenick, H. Zarabi, K. R. Thompson, V. Gradinaru, C. Ramakrishnan and K. Deisseroth, *Nature*, 2011, **471**, 358.

8 A. V. Kravitz, B. S. Freeze, P. R. L. Parker, K. Kay, M. T. Thwin, K. Deisseroth and A. C. Kreitzer, *Nature*, 2010, **466**, 622.

9 V. Gradinaru, M. Mogri, K. R. J. Thompson, M. Henderson and K. Disseroth, *Science*, 2009, **324**, 354.

10 W. R. Stauffer, A. Lak, A. Yang, M. Borel, O. Paulsen, E. S. Boyden and W. Schultz, *Cell*, 2016, **166**, 1564.

11 S. Konermann, M. D. Brigham, A. Trevino, P. D. Hsu, M. Heidenreich, L. Cong, R. J. Platt, D. A. Scott, G. M. Church and F. Zhang, *Nature*, 2013, **500**, 472.

12 R. A. Jalil and Y. Zhang, *Biomaterials*, 2008, **29**, 4122.

13 G. Chen, H. Qiu, F. Rongwei, S. Hao, S. Tan, C. Yang and G. Han, *J. Mater. Chem.*, 2012, **22**, 20190.

14 G. Chen, H. Qiu, P. N. Prasad and X. Chen, *Chem. Rev.*, 2014, **114**, 5161.

15 Z. Chen, H. Chen, H. Hu, M. Yu, F. Li, Q. Zhang, Z. Zhou, T. Yi and C. Huang, *J. Am. Chem. Soc.*, 2008, **130**, 3023.

16 F. Wang, D. Banerjee, Y. Liu, X. Chen and X. Liu, *Analyst*, 2010, **135**, 1839.

17 X. Ai, C. J. H. Ho, J. Aw, A. B. E. Attia, J. Mu, Y. Wang, Y. Wang, X. Liu, H. Chen, M. Gao, X. Chen, E. K. L. Yeow, G. Liu, M. Olivo and B. Xing, *Nat. Commun.*, 2016, **7**, 10432.

18 N. Bogdan, E. M. Rodríguez, F. S. Rodríguez, M. C. I. Cruz, A. Juarranz, D. Jaque, J. G. Solé and J. A. Capobianco, *Nanoscale*, 2012, **4**, 3647.

19 F. Vetrone, R. Naccache, A. J. Fuente, F. S. Rodríguez, A. B. Castro, E. M. Rodríguez, D. Jaque, J. G. Solé and J. A. Capobianco, *Nanoscale*, 2010, **2**, 495.

20 J. Gao, H. Gu and B. Xu, *Acc. Chem. Res.*, 2009, **42**, 1097.

21 C. H. Luo, C. T. Huang, C. H. Su and C. S. Yeh, *Nano Lett.*, 2016, **16**, 3493.

22 H. Dong, S. R. Du, X. Y. Zheng, G. M. Lyu, L. D. Sun, L. D. Li, P. Z. Zhang, C. Zhang and C. H. Yan, *Chem. Rev.*, 2015, **115**, 10725.

23 B. Ungun, R. K. Prudhomme, S. J. Budijono, J. Shan, S. F. Lim, Y. Ju and R. Austin, *Opt. Express*, 2009, **17**, 80.

24 Y. Yang, B. Velmurugan, X. Liu and B. Xing, *Small*, 2013, **9**, 2937.

25 M. M. Dcona, Q. Yu, J. A. Capobianco and M. C. T. Hartman, *Chem. Commun.*, 2015, **51**, 8477.

26 S. Jiang, Y. Zhang, K. M. Lim, E. K. W. Sim and L. Ye, *Nanotechnology*, 2009, **20**, 155101.

27 F. V. D. Rijke, H. Zijlmans, S. Li, T. Vail, A. K. Raap, R. S. Niedbala and H. J. Tanke, *Nat. Biotechnol.*, 2001, **19**, 273.

28 L. Wang and Y. Li, *Chem. Commun.*, 2006, 2557.

29 K. Kuningas, T. Ukonaho, H. Pakkila, T. Rantanen, J. Rosenberg, T. Lovgren and T. Soukka, *Anal. Chem.*, 2006, **78**, 4690.

30 T. Rantanen, H. Pakkila, L. Jamsen, K. Kuningas, T. Ukonaho, T. Lovgren and T. Soukka, *Anal. Chem.*, 2007, **79**, 6312.

31 M. Wang, W. Hou, C. C. Mi, W. X. Wang, Z. R. Xu, H. H. Teng, C. B. Mao and S. K. Xu, *Anal. Chem.*, 2009, **81**, 8783.

32 L. Mattsson, K. D. Wegner, N. Hildebrandt and T. Soukka, *RSC Adv.*, 2015, **5**, 13270.

33 Y. Min, J. Li, F. Liu, E. K. L. Yeow and B. Xing, *Angew. Chem., Int. Ed.*, 2014, **53**, 1012.

34 M. K. G. Jayakumar, N. M. Idris and Y. Zhang, *Proc. Natl. Acad. Sci. U. S. A.*, 2012, **109**, 8483.

35 H. D. Gao, P. Thanasekaran, C. W. Chiang, J. L. Hong, Y. C. Liu, Y. H. Chang and H. Lee, *ACS Nano*, 2015, **9**, 7041.

36 W. Li, J. Wang, J. Ren and X. Qu, *J. Am. Chem. Soc.*, 2014, **136**, 2248.

37 S. Shah, J. Liu, J. N. Pasquale, J. Lai, H. Mcgowan, Z. P. Pang and K. B. Lee, *Nanoscale*, 2015, **7**, 16571.

38 S. Hososhima, H. Yuasa, T. Ishizuka, M. R. Hoque, T. Yamashita, A. Yamanaka, E. Sugano, H. Tomita and H. Yawo, *Sci. Rep.*, 2015, **5**, 16533.

39 X. Wu, Y. Zhang, K. Takle, O. Bilsel, Z. Li, H. Lee, Z. Zhang, D. Li, W. Fan, C. Duan, E. M. Chan, C. Lois, Y. Xiang and G. Han, *ACS Nano*, 2016, **10**, 1060.

40 A. Bansal, H. Liu, M. K. Jayakumar, E. S. Anderson and Y. Zhang, *Small*, 2016, **12**, 1732.

41 L. Liang, A. Care, R. Zhang, Y. Lu, N. H. Packer, A. Sunna, Y. Qian and A. V. Zvyagin, *ACS Appl. Mater. Interfaces*, 2016, **8**, 11945.

42 C. Wang, L. Cheng and Z. Liu, *Biomaterials*, 2011, **32**, 1110.

43 Y. Yang, F. Liu, X. Liu and B. Xing, *Nanoscale*, 2013, **5**, 231.

44 L. He, Y. Zhang, G. Ma, P. Tan, Z. Li, S. B. Zang, X. Wu, J. Jing, S. Fang, L. Zhou, Y. Wang, Y. Huang, P. G. Hogan, G. Han and Y. Zhou, *eLife*, 2015, **4**, 10024.

45 A. D. Friedman, S. E. Claypool and R. Liu, *Curr. Pharm. Des.*, 2013, **19**, 6315.

46 K. Huang, Q. Q. Dou and X. J. Loh, *RSC Adv.*, 2016, **6**, 60896.

47 K. Cheng, S. Peng, C. Xu and S. Sun, *J. Am. Chem. Soc.*, 2009, **131**, 10637.

48 J. Xie, K. Chen, H.-Y. Lee, C. Xu, A. R. Hsu, S. Peng, X. Chen and S. Sun, *J. Am. Chem. Soc.*, 2008, **130**, 7542.

49 S. Wu and H. J. Butt, *Adv. Mater.*, 2016, **28**, 1208.

50 Z. Chen, W. Sun, H. J. Butt and S. Wu, *Chem. – Eur. J.*, 2015, **21**, 9165.

51 J. Y. Lin, *Exp. Physiol.*, 2011, **96**, 19.

52 K. Soga, K. Tokuzen, K. Tsuji, T. Yamano, H. Hyodo and H. Kishimoto, *Eur. J. Inorg. Chem.*, 2010, **2010**, 2673.

53 T. Zako, H. Nagata, N. Terada, M. Sakono, K. Soga and M. Maeda, *J. Mater. Sci.*, 2008, **43**, 5325.

54 W. C. Man, M. Miyazaki, K. Chu and J. M. Ntambi, *J. Biol. Chem.*, 2006, **281**, 1251.

55 X. Ai, L. Lyu, Y. Zhang, Y. Zhang, Y. Tang, J. Mu, F. Liu, Y. Zhou, Z. Zuo, G. Liu and B. Xing, *Angew. Chem., Int. Ed.*, 2017, **56**, 3031.

56 F. Zhang, L. P. Wang, M. Brauner, J. F. Liewald, K. Kay, N. Watzke, P. G. Wood, E. Bamberg, G. Nagel, A. Gottschalk and K. Deisseroth, *Nature*, 2007, **446**, 633.

57 M. Y. Chou, C. Y. Lee, H. H. Liou and C. Y. Pan, *Neuropharmacology*, 2014, **83**, 54.

58 A. C. Chou, Y. T. Ju and C. Y. Pan, *PLoS One*, 2015, **10**, 0138856.